

ESTIMATION OF LATERAL-DIRECTIONAL PARAMETERS FROM FLIGHT DATA USING NEURAL NETWORKS

by

SUNIL KHURCHANDANI



RE

1997

M

KHU

DEPARTMENT OF AEROSPACE ENGINEERING

EST INDIAN INSTITUTE OF TECHNOLOGY KANPUR

JANUARY 1997

ESTIMATION OF LATERAL-DIRECTIONAL PARAMETERS FROM FLIGHT DATA USING NEURAL NETWORKS

A Thesis Submitted
In Partial Fulfillment of the Requirements
for the Degree of
MASTER OF TECHNOLOGY

by
Santil Khutchandani



to the
DEPARTMENT OF AEROSPACE ENGINEERING
INDIAN INSTITUTE OF TECHNOLOGY KANPUR
JANUARY 1997

ACKNOWLEDGEMENT

I express my deep sense of gratitude to my esteemed teachers and thesis supervisors, Dr H.C. Ramaprasad and Prof. M.K. Ghosh for their invaluable guidance, constructive criticism and persistent encouragement throughout this work. I would always remain indebted to them for the precious time they have spared for me and the patience with which they always followed my path.

With all sincerity, I thank Dr P.K. Saha, the professor of Electrical Engg. Deptt. for his guidance and all the facilities he provided me for finishing my work in time.

I have no words to express my thanks to my parents and my younger who have been constant source of inspiration to me. I wish to thank all my friends and well wishers who made my stay at I.I.T.K. memorable and pleasant.

SUNIL G L

DEDICATED TO

MY FAMILY

MR. GE. BURCHAMOND

MRS. LAYLA ELIN BURCHAMOND

KASHALL, HOME AND HEATH

ABSTRACT

Application of Fast Forward Neural Network (FFNN) to Aerodynamic Engineering problem is one of the current topics of interest. The FFNNs do not require an a priori model of aircraft for modeling, and provide a black - box type of model of the aircraft by mapping suitable network inputs to chosen network outputs. The present thesis deals with modeling of aircraft lateral-directional dynamics through FFNNs and application of recently proposed Delta-method for the estimation of aircraft stability and control derivative (parameters). For modeling aircraft motion variables and the control inputs are used as the input file while aerodynamic force or moment coefficients are used as the output file for training FFNN. For the purpose of parameter estimation, the trained FFNN is now presented with suitably modified input file and the accompanying predicted output files of force and moment coefficients are obtained. Suitable interpolation and processing of these input-output files results in estimated values of the parameters. The method is verified on lateral-directional simulated flight data. A detailed study has been carried out to show how the accuracy of estimates gets affected when flight data corresponding to various types and forms of aileron and/or rudder control inputs are analysed. It is shown that the combination of aileron and rudder applied in certain sequential form leads to better estimates. Finally, it is also shown that the Delta-method is quite robust and can be used for parameter estimation even if flight data contains measurement noise.

CONTENTS

ABSTRACT

List of Figures

List of Symbols

CHAPTER	TITLE	Page No.
1	INTRODUCTION	1
2	FEED FORWARD NEURAL NETWORKS	9
3	SIMULATED FLIGHT DATA GENERATION AND THE METHOD USED	18
4	RESULTS AND DISCUSSION	22
5	CONCLUSION AND RECOMMENDATIONS	24
	REFERENCES	24
	TABLES	43
	FIGURES	50

LIST OF FIGURES

Serial Number	Page Number
1. Figure of a wing	5
2. Figure of FHM with two rolling layers	10
3. Figure Showing Aircraft Axis System	11
4. Three Types Of Control Input Forms	12
5. Figure of Pulse type control input (case VI)	13
6a. Figure of multistep 2-2-1-1 attack input signal (case VII)	14
6b. Figure of multistep 2-2-1-1 roller input signal (case VII)	15
7a. Comparison Of Actual, Trained and Estimated Response Of Rolling Moment Coefficient (C_{l1})	16
7b. Comparison Of Actual, Trained and Estimated Response Of Yawing Moment Coefficient (C_{l2})	17
7c. Comparison Of Actual, Trained and Estimated Response Of Force Coefficient Along Y-axis (C_{y1})	18
8a. Histograms For Estimated Parameters C_{l1p} , C_{l1r} , C_{l2p} , C_{l2r} and C_{y1p}	19
8b. Histograms For Estimated Parameters C_{y1r} , C_{y2p} , C_{y2r} , C_{y3p} and C_{y3r}	20
8c. Histograms For Estimated Parameters C_{y4p} , C_{y4r} , C_{y5p} , C_{y5r} and C_{y6r}	21

LIST OF SYMBOLS

SYMBOL

1

C_1	rolling moment coefficient
C_R	pitch moment coefficient
C_{Y_2}	force coefficient along Y axis
D	drag force function
I_{yy}	moment of inertia about X-axis, kg-m ²
S	reference area, m ²
M_2	velocity, m/sec
b	span, m
f	nonlinear sigmoidal activation function
m	aircraft mass, kg
n_1	number of nodes in input layer
n_h	number of nodes in hidden layer
n_o	number of nodes in output layer
r	roll rate, rad/sec
r	yaw rate, rad/sec
s	half the span, m
w	weight matrix between two layers
\hat{y}	estimated output
y	desired output
β	sideslip angle, deg or rad
δ_n	aileron deflection, rad
δ_r	rudder deflection, rad
g	gravity gain or step factor
μ	learning rate parameter

SuperScript

derivative with respect to time

T

transpose of matrix

Stability And Control BookList

$$C_{1p} = \partial C_1 / \partial (p_1 / \partial U_1) \quad , \quad C_{1q} = \partial C_1 / \partial (q_1 / \partial U_1) \quad , \quad C_{1r} = \partial C_1 / \partial (r_1 / \partial U_1) \quad ,$$

$$C_{2p} = \partial C_2 / \partial (p_2 / \partial U_2) \quad , \quad C_{2q} = \partial C_2 / \partial (q_2 / \partial U_2) \quad , \quad C_{2r} = \partial C_2 / \partial (r_2 / \partial U_2) \quad ,$$

$$C_{3p} = \partial C_3 / \partial p \quad , \quad C_{3q} = \partial C_3 / \partial q \quad , \quad C_{3r} = \partial C_3 / \partial r$$

$$C_{1,p_1} = \partial C_1 / \partial p_1 \quad , \quad C_{1,q_1} = \partial C_1 / \partial q_1 \quad , \quad C_{1,r_1} = \partial C_1 / \partial r_1$$

$$C_{2,p_2} = \partial C_2 / \partial p_2 \quad , \quad C_{2,q_2} = \partial C_2 / \partial q_2 \quad , \quad C_{2,r_2} = \partial C_2 / \partial r_2$$

INTRODUCTION

The process of estimating numerical values of aerodynamic stability and control derivatives (parameters) from flight test data is termed as Parameter Estimation. The mathematical model representing airplane dynamics requires accurate values of these parameters. Such mathematical models are useful for verification of stability augmentation system (SAS) and in-flight monitoring.

Three distinct approaches for estimating these stability and control derivatives are

- (i) Theoretical Methods
- (ii) Wind Tunnel Testing
- (iii) Flight Testing

At initial design stages of aircraft design, theoretical methods¹⁻³ provide the only reasonable way of estimating the aircraft parameters. However the accuracy of such theoretical estimates being not as high, there is need to verify these estimates with those obtained from wind tunnel testing and flight testing. Wind tunnel methods although improve accuracy of estimation of parameters, they are time consuming and expensive. Further, simulation of control surfaces, power effects and various flight conditions are difficult to simulate satisfactorily. Wind tunnel estimates also suffer from discrepancies due to interference effects of support system, wall effects, turbulence level etc. It is, therefore, desirable that the wind tunnel estimates be corroborated with estimates from wind flight test data.

Three popular methods to estimate statistical test-control derivatives from flight test data are as follows :

- (i) Equation Error Method
- (ii) Output Error Method
- (iii) Maximum Likelihood Method

The principle of least squares is used in Equation Error Method. The error gets minimized with respect to unknown parameters in each of the equations. Its advantages include computational simplicity, non-iterative nature and applicability to both linear as well as nonlinear models. However this method can not be applied if all the states are not measured accurately and gives poor results if measurements are noisy. Thus in order to get accurate results model errors are required for data reconstruction and smoothing. Since then these data processing tasks are more complicated than the task of parameter estimation itself. The errors between the measured and model response produced by identical inputs is minimized by Output Error Method. The method assumes that there exist no modeling errors. The method processes the measured data while smoothing the model representation of given system to be error. A comprehensive survey of these methods is reported by Stein and GH⁴. The methods like model matching⁵, Newton-Raphson Method⁶, Modified Newton-Raphson method⁶ etc. fall in this category.

Maximum Likelihood⁷ estimators are those for which the observed value would be the most likely to occur. The main advantage of this method is that estimated parameters are asymptotically

approximation which can collectively model any nonlinear relationship between the inputs and the outputs.

ANN can only operate with given input-output data. Some networks require only input variations and are called as auto associative networks while others require input-output pairs and are called as hetero associative networks.

Nodes or neurons are the units where all the computations are performed. Figure 1 illustrates the most common type of neuron. Each neuron collects information from incoming connections and produces single output value. ANNs also consist of sigmoid/transferal between the nodes which not only allow information to flow in particular defined direction but also assign weight to the information. Such connection weights are termed as synaptic weights. These weights are adjusted by accordance to a well defined algorithm which helps to capture knowledge within the network.

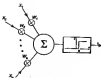


Figure 1 – Single Neuron

Due to the above properties, ANNs are widely preferred for mapping any unknown relationship between the input and output. It can be stated that it is a black box model structure because functional relationship between the input and output is not explicitly known.

There are several types of ANNs, but only two of them have especially found application in the field of aircraft system identification. These are -

(i) Feed Forwarded Neural Network (FFNN)

(ii) Recurrent Neural Networks (RNN)

FFNNs lead to a black box model in which no physical significance can be added to either network structure or to the network weights.^[3-11] RNNs have fixed structure and possess fixed number of nodes equal to number of unknown parameters.

FFNNs have neurons arranged in layers like directed graphs, and they are stable in nature. RNNs are dynamic neural networks incorporating an output feedback, as neural paper flow and respiration^[12] have shown. Availability of RNNs to state space modeling and thereby demonstrated their applicability to explicitly estimate aircraft parameters. However as pointed by authors^[8] it has been only a limited scope for aircraft identification applications and it is the FFNNs which may prove to be more flexible and thereby have higher potential for future applications for modeling aircraft dynamics and aircraft parameter estimation.

Recently, system identification has been re-examined by using

researchers using FNN^{[1]-[3]}. Significant contributions in this direction have been made by Hsu^[1], Tsao^[2] and Hong^[3], Sussangkarn and Jitapantakul^[4], Kari and Jitapantakul^[5], and Lator and Granga^[6]. Hsu^[1] dealt with use of FNNs to represent aircraft aerodynamics. Tsao^[2] et al.^[2] demonstrated the feasibility of neural modeling approach to establish a nonlinear aerodynamic model that is amenable to flight test data processing. Sussangkarn and Jitapantakul^[4] have studied various aspects of FNN modeling and its applicability to real flight data. Kari and Jitapantakul^[5] have shown use of FNN for aircraft parameter estimation. Lator and Granga^[6] have shown accurate modeling of aerodynamic coefficients using a system identification model composed of an extended Kalman-Bucy filter for state and force estimation and a computational neural network for aerodynamic model.

In a recent paper Polingphol et al.^[7] have proposed two new methods for estimation of airplane parameters using FNNs. The proposed methods are called Delta method and Zero method. Both methods have been validated on simulated flight data generated for longitudinal dynamics of an example aircraft. Out of these two, Delta method was shown to be more reliable, consistent and robust. We have therefore, chosen Delta method for present study wherein its applicability to extract lateral-directional stability and control parameters from flight data to explore systematically following aspects of application of FNNs to aircraft lateral-directional dynamics are dealt with.

(i) Aerodynamic modeling of lateral-directional dynamics using

ITNN wherein input and output coefficients C_1, C_2, C_3 are mapped to neuronal system variables p, r, δ and control inputs δ_u, δ_r . Various aspects about simulating variable ITNN structure and associated network parameters like learning rate, momentum rate, slope etc. are studied.

1.2.4 Application of Delta-method for estimating lateral-directional parameters from simulated flight data for an example aircraft is demonstrated. A detailed study has been carried out to show how accuracy of estimates is affected by the type of control input used for generating flight data. Results are also presented to indicate the effect of measurement noise present in the simulated flight data on the accuracy of estimates.

The layout of the present work is as follows:

After introduction in chapter one, details of ITNN and backpropagation algorithm are given in chapter two. Chapter three deals with the method used for parameter estimation and various aspects about the generation of simulated flight data. Chapter four consists of descriptive study of the results obtained. Lastly, chapter five briefly shows the conclusions drawn on the basis of results obtained and also shows the recommendations for future work.

CHAPTER 2

FEED FORWARD NEURAL NETWORKS

2.1 General

2.2 Backpropagation

2.2.1 Initialization of Weights

2.2.2 Forward Propagation

2.2.3 Backward Learning Algorithm

2.3 Modeling Prediction and Influence

Parameters of FFNN

2.1 General

FFNNs are multi-layered perceptrons consisting of an input layer, an output layer and one or more hidden layers. The number of neurons/units in the input layer and the output layer are determined respectively by the number of input and output variables while the number of neurons in the hidden layer(s) is dictated by the complexity of the problem. Figure 1 shows a general schematic picture of FFNN with two hidden layers consisting of many neurons.

FFNNs are static and characterized by unidirectional flow of variables i.e. the inputs are propagated through the hidden layers to the output layer. Each node in the input/output or hidden is connected to each node in the next layer/unit(s) the hidden or the output through a connection weight. Every node in the input layer and the hidden(s) layer is biased. The nodes in the hidden layer(s) and the output layer have a nonlinear activation function, e.g., sigmoidal or hyperbolic tangent function. The hidden nodes in FFNN have good approximation capability and thereby allow the network to build a model of arbitrary complexity between the input(s) and the output(s).

For specific case of aircraft's lateral-directional dynamics, the input variables to the network are the motion variables y, r, β and the aircraft control input signals δ_a , δ_r or δ_s while the output variable is yaw/roll force or moment coefficient Y_r .

weight descent coefficient(Δw_{ij}), or rolling descent coefficient(Δw_{ij}), or first coefficient along a axis(Δw_{ij}). Figure 3 shows fully feed back system. The known input-output data is first used to train the network. The predicted output values of \hat{C}_1 , \hat{C}_2 , \hat{C}_3 are compared with the corresponding known values of C_1 , C_2 or C_3 and the errors are backpropagated using a method called the back propagation algorithm (BPA). This process results in updating of network connection weights. The training of the network is continued till the mean square error (MSE), defined as follows, is less than the prescribed value.

Mean square error (MSE) defined by equation (6) is used to test the convergence the influence parameters are varied until the MSE is within the defined limits -mean square error can be expressed as [10]

$$MSE = \frac{1}{Nn} \sum_{i=1}^N \sum_{j=1}^n (y_j(i) - \hat{y}_j(i))^2 \quad (6)$$

where, N is the number of data points, n is the number of input variables, y is the desired or associated response and \hat{y} is the calculated response of the network.

The details of BPA and forward propagation in FNN are described next.

3.2 Backpropagation Algorithm (BPA)

Backpropagation⁸ is a simple iterative gradient descent algorithm. The essential idea behind the BPA, which is widely

used for training multi-layered perceptrons, is to view the cost function as a function of network weights or parameters, and the perform gradient descent in the weight parameter space to search for a minimum error between desired and estimated value. In this method, weights are updated incrementally so that, at each iteration a small step is taken in the negative direction of the error to make it small more rapidly.

There are two common types of BPN learning algorithms :

- Batch or Group BPB
- Sequential or Iterative BPB

The batch BPB updates the network weights after presentation of the complete training data set. Hence, a training iteration incorporates one sweep through all the training patterns.

In case of recursive BPB, also called pattern learning, the network weights updated sequentially as the training data set is presented. The recursive BPB is more convenient and efficient as compared to the batch BPB.

A brief summary of the BPB algorithm for one hidden layered PPNB is given below for completeness.

3.2.3 Initialization of Weights

The input and output weight matrices of the network are initialized randomly. With reference to Figure 2, the order of weight matrices and weight vector is as follows :

Matrix/Vector	Symbol	Order of matrix/vector
(a) Weight matrix between input and hidden layers	w_1	$n_1 \times n_2$
(a) bias weight vector	w_{10}	$n_1 \times 1$
(a) weight matrix between hidden and output layer	w_2	$n_2 \times n_3$
(a) bias weight vector	w_{20}	$n_2 \times 1$

where n_1 , n_2 and n_3 are the number of nodes in the input , hidden and output layers respectively .

2.1.2 Forward propagation

During the forward propagation , for a given input vector x_0 , the calculated output vector y_1 is computed

(i) Propagation from input layer to hidden layer

$$x_1 = w_1 \times x_0 + w_{10} \quad (2a)$$

$$y_1 = f (x_1) \quad (2b)$$

where x_1 is the vector of intermediate variables , y_1 is the vector node output at the hidden layer and f is the vector of nonlinear sigmoidal node activation function , defining the node characteristic

It should be noted that each component of the vector on left hand side corresponds to the respective component of the vector on right hand side for all the equations

The sigmoidal function may be written as,

$$f_j(x_j) = \frac{1}{1 + e^{-x_j/\theta_j}} \quad j=1,2, \dots, n_2 \quad (3)$$

where λ is the logistic gain or slope factor of the hidden layer activation function. All the nodes of any particular layer have, generally, the same slope factor.

(ii) Propagation from hidden layers to output layer:

$$x_2 = w_2^T \cdot y_1 + w_{20} \quad (14)$$

$$u_2 = f(x_2) \quad (15)$$

where x_2 is the vector of intermediate variables, y_1 is the vector node output at the output layer and f is the vector of nonlinear sigmoidal node activation function.

Similarly, the sigmoidal function in this case is

$$f_j(x_2) = \frac{1}{1 + e^{-\lambda(x_2 - x_{20})}} \quad \text{for } j = 1, 2, \dots, n_2 \quad (16)$$

3.2.3 Recursive Learning Algorithm

The backpropagation learning algorithm is based on optimizing a suitably defined error cost function. At each point the local output error cost function, which is sum of squared errors, is given by

$$E_k = \frac{1}{2} \cdot (z - u_2)^T (z - u_2) \quad (17)$$

where k is the discrete time data index, z is the measured response vector, u_2 is the network estimated response vector and $e_k = [z - u_2]$ denotes the error.

Minimization of eq.(17), applying the steepest gradient descent method, also called delta rule, yields

$$\mathbf{w}_2^{(k+1)} = \mathbf{w}_2^k + \mu \cdot (1 - \delta) \nabla_{\mathbf{w}_2} \ell(\mathbf{w}_2) \quad (3)$$

where $\mu \in [0, 1]$ is learning rate parameter. Decreasing the speed of convergence, $(1 - \delta) \nabla_{\mathbf{w}_2} \ell(\mathbf{w}_2)$ is the gradient of error cost function with respect to \mathbf{w}_2 . A proper choice of learning rate parameter, μ , is necessary to ensure reasonable convergence rate.

Partial differentiation of eq.(3) with respect to the elements of weight matrix \mathbf{w}_2 and substitution of Eqs. (4a) & (4b) yields gradient of the error cost function

$$(1 - \delta) \nabla_{\mathbf{w}_2} \ell(\mathbf{w}_2) = -f'(x_2) \cdot (1 - a_2) \cdot \mathbf{w}_2^T \quad (5)$$

where $f'(x_2)$ is the derivative of the output node activation function i.e. eq. (2).

Defining r_{20} as,

$$r_{20} = f'(x_2) \cdot (1 - a_2) \quad (6a)$$

and by adding momentum term in Eq. (7), the weight update rule for the output layer is obtained as

$$\mathbf{w}_2^{(k+1)} = \mathbf{w}_2^k + \mu r_{20} \cdot \mathbf{w}_2^T + \delta \cdot (\mathbf{w}_2^k - \mathbf{w}_2^{(k-1)}) \quad (6b)$$

where δ is momentum term.

Over relaxation of the gradient update i.e. of \mathbf{w}_2 (7), through the last term on the right hand side of eq. (7), called momentum term, helps to damp out the periodic oscillations in the weight update, e.g., due to large value of learning rate, μ approximately 1. It amounts to increasing the learning rate from μ to $\mu \cdot (1.0 - \delta)$ without resupplying the periodic oscillations.

Similarly, the partial differentiation of eq. (8) with respect to \mathbf{w}_1 and substitution of eq. (2a) & (2b) yields

$$(1 - \delta) \nabla_{\mathbf{w}_1} \ell(\mathbf{w}_1) = -f'(x_1) \cdot a_2^T \cdot r_{10} \cdot \mathbf{w}_1^T \quad (8a)$$

where $f'(x_j)$ is the derivative of hidden layer activation function : σ of eq. (2)

$$w_{20} = f'(x_j) \cdot w_2^B \cdot w_{20} \quad (10c)$$

The weight update rule for the hidden layer is given by

$$w_j^{(k+1)} = w_j^k + \eta \cdot w_{20} \cdot w_2^T \cdot \eta \cdot (w_4^k - w_1^B \cdot w_j) \quad (11)$$

For the sigmoid function its equivalent right column respectively on the hidden and output layer node activation function respectively , the derivatives $f'(x_1)$ and $f'(x_2)$ are given by

$$f'(x_j) = \frac{-i \cdot p \cdot (1-i)}{1 + e^{-i \cdot p \cdot (1-i)}} \quad (12)$$

It may be pointed out that the training algorithm is recursive . as stated above , the weights are updated repeatedly for each time point using eqs (8 & 12)

From computational view point, the backpropagation algorithm (BPA) requires

- (i) Computation of the hidden & output node activation function i.e. eqs (2a & (2b) and eqs (3a & (3b)
- (ii) Computation of the error cost function i.e. eqs (4a & (4b)
- (iii) Computation of the derivatives of the node activation function is Eq.(12) for hidden and output layer
- (iv) Computation of the new weights from Eqs. (5 & (6) until the desired accuracy is obtained

3.3 Modeling, Feedforward and Influence Parameters of FFNN

An initial network problem solving using FFNN consist of two

phases , namely (i) learning or training phase and (ii) prediction phase

In modeling , learning or training phase procedure consists of presenting the known input and output data to network and adjusting the network weights using backpropagation algorithm (BPA). During this procedure network captures the functional relationship existing between the inputs and outputs that necessarily is the same there as in the original physical model in form of network weights . Once modeling or training is over and network weights and topology is known , the same data is passed through the network with the same topology to check for prediction capability of the network based on some performance criteria (MSE in the present study) .

There are several network parameters which affect the convergence rate . These influence parameters are

1. Number of Hidden Layers (H.L.)
2. Number of neurons in each hidden layer (n's)
3. Learning Rate Parameter (α)
4. Momentum Rate Parameter (β)
5. Number of Iterations (I)
6. Initial Network Weights (I.N.W.)
7. Weight Limit.
8. Logistic Sigmoid slope Factor (δ)

Determination of optimal topology is a cumbersome job . It is hit and trial method which is like pure science and pure art . In standard literature on ITNN , some heuristic rules have been proposed

for structure and parameters of LSTM's for various applications. One has to still develop one's own set of thresholds by repeated trials of training the network for the problem at hand. We have found and experimented a set of values of various parameters for mapping lateral-directional dynamics of an aircraft. These values are presented in chapter four.

CHAPTER 3
PARAMETER ESTIMATION METHODS
AND
SIMULATED FLIGHT DATA GENERATION

3.1. General

3.2. Data-method

3.3. Simulated Data Generation

3.4. Examples of Motion

2.1 General

In this chapter, we first describe the subject features of *Data-method^{DT}* used for parameter estimation from flight data using Feed Forward Neural Networks that we called the procedure used and term of simulated data generated for analysis via *Data-method*. Details of the sample airplane used and types of control inputs utilized for generating simulated flight data are also given. Flight data with and without pseudo measurement noise were prepared for analysis-although real flight data for lateral-directional dynamics of an airplane were recently obtained and are being separately analyzed by others, we did use the control input term used for real flight data to generate corresponding simulated flight data for analysis and comparison with the results obtained by others. Scarcity of time did not permit analysis of the complete real flight data to be included in the present work.

2.2 Data-method

Parameters occurring in the equations of motion of an aircraft represent partial derivatives of aerodynamic forces and moments coefficients with respect to the corresponding motion or control input variables. In other words these parameters can be thought of as variation in aerodynamic coefficients due to small

variation is

one of the network or control variables about the nominal value in such a way that only that particular variable is allowed to change while rest of the variables are held constant at their nominal values. This constrained perturbation is employed to derive sensitivity for estimating aircraft parameters.

Let us now assume that ITNN is already trained to map the network input variables p, r, δ, δ_R and δ_L to the output variables $\dot{\delta}_p$ or \dot{C}_{δ_R} or \dot{C}_{δ_L} ... Now only one of the network inputs is given a small(δ), perturbation at each time point while all others are held at their original values. Such a modified input file is now presented to the trained neural network to predict the perturbed value of aerodynamic coefficients at the output node. The difference in the predicted value of aerodynamic coefficient from the value predicted for the original values of inputs is due to the perturbation in the value of the chosen network input variable. The difference so calculated in the value of aerodynamic coefficient divided by the perturbation value yields the corresponding network's parameter. For example say δ is perturbed by small value $\delta\theta$ and difference observed in the predicted value of \dot{C}_{δ} for δ and $\delta+\delta\theta$ is $\Delta\dot{C}_{\delta}$. Then $\Delta\dot{C}_{\delta}/\delta\theta$ yields the stability derivative $\dot{C}_{\delta\theta}$. Similarly perturbation in δ_R and corresponding $\Delta\dot{C}_{\delta_R}$ observed will yield scaled derivative $\dot{C}_{\delta_R\delta_R}$ where $\dot{C}_{\delta_R\delta_R} = \Delta\dot{C}_{\delta_R}/\delta\theta$. To avoid bias due to one sided differences, positive and negative variation are perturbed in both increasing and decreasing direction. For example \dot{C}_{δ} values for $\delta+\delta\theta$ and $\delta-\delta\theta$ are predicted

to be \hat{C}_Y^L and \hat{C}_Y respectively, then $\hat{C}_{\hat{Y}} = \hat{C}_Y^L = \hat{C}_Y^U / \log 2$.

It should be noted that for each of the perturbed values at each test point, there will be a corresponding predicted value of aerodynamic coefficient, and hence a different estimated value of the parameter estimate. Ideally all such values should have been identical to yield a single value of the parameter. However, by seeing there is variation in predicted values. Histograms of all the estimated values showed a near normal distribution. Thus the mean value is used as the estimate and standard deviation, about the mean as the measure of accuracy of the estimates.

3.3 Simulated Data Generation

In the absence of real flight data, simulated data is used as the input-output data to train the LSTM. This simulated data is obtained by solving the lateral-directional equations of motion for an example aircraft. For the present study the example aircraft was chosen to be the DAR research aircraft ACT6, details of which are given in the DAR report by Jategaonkar¹⁸. This aircraft was chosen as real flight data for it was acquired recently and was being analysed by others. Thus it would help comparison with results from real flight data at a later date. Also, we could utilize the control input from used for real flight and we have analysed the corresponding simulated data for parameter estimation. For generation of simulated data equations of motion used are given next.

3.4 Equations of Motion

For generation of lateral-directional simulated flight data, following perturbed equations of motion⁽²⁸⁾ are used,

$$\dot{u} = -u \dot{V}_T + p \cos \theta + q \sin \theta \quad \cos \theta = \frac{V}{V_T} \sin \alpha \quad \dot{V}_T = 0 \quad (32a)$$

$$\dot{w} = -p \sin \theta + q \dot{V}_T + \dot{q} \sin \theta \quad \cos \theta = \frac{V}{V_T} \sin \alpha \quad \dot{V}_T = 0 \quad (32b)$$

$$\begin{aligned} \dot{p} = & \frac{1}{I_{xx}} \left(\frac{1}{2} \rho V^2 S_{ref} l \left(C_{l\dot{\alpha}} C_{l\beta} + C_{l\dot{\beta}} C_{l\alpha} \right) + \frac{1}{2} \rho V_{T0}^2 S_{ref} l \left(C_{l\dot{\alpha}} C_{l\beta} + C_{l\dot{\beta}} C_{l\alpha} \right) \right) \\ & - (32c) \end{aligned}$$

$$\begin{aligned} \dot{r} = & \frac{1}{I_{yy}} \left(\frac{1}{2} \rho V^2 S_{ref} l \left(C_{l\dot{\alpha}} C_{l\beta} + C_{l\dot{\beta}} C_{l\alpha} \right) + \frac{1}{2} \rho V_{T0}^2 S_{ref} l \left(C_{l\dot{\alpha}} C_{l\beta} + C_{l\dot{\beta}} C_{l\alpha} \right) \right) \\ & - (32d) \end{aligned}$$

$$\dot{\beta} = \dot{p} + q \sin \theta \sin \theta + r \cos \theta \sin \theta \quad (32e)$$

$$\dot{\alpha} = \dot{q} \cos \theta + r \sin \theta \quad (32f)$$

where,

$$\beta = u/V_T, \quad \dot{\beta} = \frac{1}{V_T} \frac{d\beta}{dt}$$

$$C_{l\dot{\alpha}} = C_{l\dot{\alpha}}(\beta u/V_T) + C_{l\dot{\alpha}}(\beta u/V_T) + C_{l\dot{\alpha}}\beta + C_{l\dot{\alpha}}\dot{\beta} + C_{l\dot{\alpha}}\dot{r} \quad (33a)$$

$$C_{l\dot{\beta}} = C_{l\dot{\beta}}(\beta u/V_T) + C_{l\dot{\beta}}(\beta u/V_T) + C_{l\dot{\beta}}\beta + C_{l\dot{\beta}}\dot{\beta} + C_{l\dot{\beta}}\dot{r} \quad (33b)$$

$$C_{l\dot{\alpha}} = C_{l\dot{\alpha}}(\beta u/V_T) + C_{l\dot{\alpha}}(\beta u/V_T) + C_{l\dot{\alpha}}\beta + C_{l\dot{\alpha}}\dot{\beta} + C_{l\dot{\alpha}}\dot{r} \quad (33c)$$

The steady flight conditions, which the perturbations are indicated, mass moment of inertia, and geometric measure of the aircraft, taken from reference⁽²⁸⁾, are as follows

$$V_T = 100.0 \text{ m/sec}^2$$

$$W = 1000.0 \text{ N}$$

$$g = 9.81 \text{ m/sec}^2$$

$$\rho = 0.78 \text{ kg/m}^3$$

$$S = 16 \text{ m}^2$$

$$l = 3.00 \text{ m}$$

$$b = 25.5 \text{ m}$$

$$\begin{aligned} I_{\text{ax}} &= 14333.2 \text{ kg-m}^2, & I_{\text{yy}} &= 252677.6 \text{ kg-m}^2 \\ I_{\text{ay}} &= 238960.97 \text{ kg-m}^2, & I_{\text{xx}} &= 187633.6 \text{ kg-m}^2 \end{aligned}$$

where U_0 is the velocity, ρ is density of training aircraft of aircraft under consideration, b is the span, y is mean aerodynamic chord, Q is reference area and P_y are the moment of inertia about the specified axis.

Fourth order Runge-Kutta method is used to solve above set of equations for generating series variables $p(t), r(t), q(t)$ for each known control input, form of $\delta(t)$ and $\delta(t)$. The network input file is prepared using these values of q, r, p, δ and δ . The force and moment coefficients, $C_L, C_D, C_Y, C_L, C_Y, C_D$ are calculated from eq (14)-(16) and these form network output variables. For simulated flight data, true values of the parameters given in Table 1 were fed into the above set of equations Eqs (14)

CHAPTER 4

RESULTS AND DISCUSSION

RESULTS AND DISCUSSION

Simulated flight data for lateral-directional dynamics of an aircraft were generated for different configurations of control and sensor control system. The network takes the measured of sensor variables (input) along with aircraft control inputs (its output) (ii). The network output file was either C_{L_0} or C_{L_0} or C_{L_0} . The network was trained using each input-output files for many sets sets of simulated flight data. The network tuning parameters were varied to obtain the optimal architecture that was used for parameter estimation for all the sets of flight data. To this purpose selected parameters were varied in the range shown below. The final values selected for the present study are also shown below in the third column.

Network Parameter	Range of variation tried	Final Value
Logistic Gain	0.01-0.0	0.05
Random Seed	0.0-0.0	0.4
Number of Hidden Layers	1-3	1
Number of Nodes in Hidden Layer	0-10	8
Number of Iteration	2000-10000	10000
Learning Rate	0.3-0.0	0.3
Minimum Error	0.4-0.0	0.0

The criterion for selection of network parameters was based on MSE observed at the end of selected number of iterations. It was found that MSE decreased up to about 1000 iterations, and beyond it, the decrease was marginal. To save on computational

used, for all the further studies the architecture along with number of iterations was kept fixed as 5000. Although it is possible that slight variations in the network parameters may result in lower MSE for specific set of flight data, it was decided to freeze the architecture of network for all studies reported British due to limitation of time. Since present work is concerned with parameter estimation via Delta method, we refrain from reporting detailed discussion on training phase and effects of network parameters on the MSE, and thereby on the match obtained between the desired and the predicted values of C_L or C_D or C_Y . The effect of network parameters on training was similar to that reported in the literature, i.e., Bannan and Ingham¹⁴ and Ehsan Kiani¹⁵.

As reported in literature, multimap 2-2-4-4 type of control inputs have been found very efficient for generation of flight data to be used for parameter estimation. A multimap 2-2-4-4 type of input consists of control deflection for δ_a and δ_r second in $+ve$, $-ve$, $+ve$ and $-ve$ direction respectively. The maximum magnitude was kept at 0.1 or 0.05 radians, and duration was seven seconds. To bring out the relative merits of 2-2-4-4 type of input, it was of interest to explore parameter estimation using flight data for other type of control inputs. Two such control inputs, namely an arbitrary and a sinusoid (Fig.4) were used for flight data generation. For each a comparative study following five types of control inputs were used to obtain corresponding flight data for parameter estimation via Delta method.

- case I : Maneuver 3-3-3-1, elevator input, maximum amplitude 0.1 radians and duration seven seconds.
- case II : Maneuver 3-3-3-1, aileron input, maximum amplitude 0.1 radians and duration seven seconds.
- case III : An arbitrarily varying elevator control input, with maximum magnitude 0.1 radians and duration seven seconds.
- case IV : A sinusoidal elevator input, of maximum amplitude 0.1 radians and duration seven seconds.
- case V : Combination of identical maneuvers 3-3-3-1, elevator and aileron control inputs. Both having maximum amplitude as 0.1 radians and duration seven seconds.

Using these different inputs, the simulated flight data was generated and parameters were estimated via Delta method. The results corresponding to case I - V are listed respectively in columns 3 - 7 of Table 4, along with true values of parameters in column 8 for ready comparison.

case I (Table 4, column 3) : As seen from Table 4, except for $C_{L_{\delta e}}$ and $C_{L_{\delta a}}$, all the other parameters are well estimated. However, values of standard deviation for some of the parameters are on higher side. Further, control derivatives like $C_{L_{\delta e}}$, $C_{L_{\delta a}}$, $C_{Y_{\delta e}}$ cannot be estimated since there is no aileron input available in the current input. The fit for perturbation is captured by Delta method.

case II (Table 4, column 4) : Results for fit show some degradation as compared to those for fit done comparison with 3rd

values least it shows that, in addition to \hat{C}_{py} , \hat{C}_{pr} as case 1 \hat{C}_{ap} , \hat{C}_{ap} and \hat{C}_{ap}^2 are poorly estimated. Again, control derivatives for states $\{C_{\text{lat}}, C_{\text{lat}}^2, C_{\text{lat}}^3\}$ can not be estimated for this case, more so as it is available in network input file.

case III (Table 1, column II) - Compared to case 1, the arbitrary dc control input results showed disturbance in estimated values, specially in \hat{C}_{ap} , \hat{C}_{ap} and \hat{C}_{ap} values while \hat{C}_{py} and \hat{C}_{pr} estimates remained poor as in case 1. Thus combining 2-D-cd input signal seems to be superior over the arbitrary input signal.

case IV (Table 1, column III) - The parameter estimation were poor except for β -derivatives ($\hat{C}_{\text{py}}, \hat{C}_{\text{ap}}, \hat{C}_{\text{ap}}$) as compared to the cases discussed above. This is due to the fixed frequency of the sinusoidal signal which is unable to excite all the modes of the aircraft dynamics.

case V (Table 1, column VI) - All the above cases had only one of the controls (ls or lr) used for exciting aircraft dynamics and thereby we could estimate only the corresponding control derivatives, i.e., either ls or lr. Simultaneous, identical ls and lr inputs were used for generating flight data and so control derivatives for both ls and lr could be estimated by permuting them in network input file. Estimates from this data showed that like previous cases, \hat{C}_{py} and \hat{C}_{pr} were still being poorly estimated and estimates for both ls and lr ($\hat{C}_{\text{lat}}, \hat{C}_{\text{lat}}^2, \hat{C}_{\text{lat}}^3, \hat{C}_{\text{lat}}, \hat{C}_{\text{lat}}^2, \hat{C}_{\text{lat}}^3$) were also poor. A close scrutiny of the estimated values of these control derivatives showed that there was a pair-wise high correlation between $\hat{C}_{\text{lat}}, \hat{C}_{\text{lat}}$.

$(C_{y\dot{\delta}_a}/C_{y\dot{\delta}_a})$ and $(C_{y\dot{\delta}_a}/C_{y\dot{\delta}_a})$ is the case that both the control derivatives of the pair had almost equal values. Initially this result looked very strange but on reflection it was clear that indeed the values should be either exactly equal or almost equal to one the case. The reason for expecting such equal values is for both in that we are showing the neural network two identical inputs, namely δ_a and $\dot{\delta}_a$ and they are indistinguishable from neural network point of view. It is like showing the same input twice to neural network.

The state observation required a network at the type of control inputs to be used for generating flight data so as to enable estimation of all the stability and control derivatives with better accuracy. As a first step we used the real control inputs that has been used in generating real flight data provided by IIR Company. We could not analyze the state set of this real flight data as these were received very late when the thesis work was nearing completion. Analysis of complete data set is being carried out by another Ph.D. candidate.

From the data set supplied we chose two types of control inputs forms which are put under case VI and case VII

case VI : Pulse type aileron input (Fig.5)

case VII : Combination combination 2-2-2-1 type aileron and rudder inputs (Fig.6a and 6b)

Using these control inputs, simulated data was generated and parameters estimated via Delta method. The results for these 180 cases are given in table 2 and discussed below :

case VI (Table 2, column 2) - In general, the estimated parameters compared well with the true values, except that the roller control derivatives still could not be estimated and derivatives like $C_{\dot{\delta}_r}$, $C_{\dot{\delta}_r}$, and $C_{\dot{\delta}_r}$ were not well estimated.

case VII (Table 2, column 4) - Estimated parameters in this case showed remarkable improvement in their estimated values when compared with case V. Here not only were both roller derivatives estimated separately but also their estimated values were close to the true values, and standard deviations were extremely low. On the whole, all the parameter estimates showed better comparison with the true values.

In the face of it, such improved results were surprising and it was first suspected that this could be due to measurement noise that may be present in the control inputs applied but from the real flight data. Alternatively, it was conjectured that this may be due to the roller and aileron inputs being not identical as was the case for case V. Thus, the real control inputs may have contained measurement noise and would not have identical shape. To test this conjecture, flight data was generated for δ_a and δ_r combination where both δ_a and δ_r inputs had certain pseudo measurement noise added to them. Specifically pseudo measurement noise of 15 and 10 was added to the control inputs that were used in case V in combination of subcases 3-2-1-1 δ_a and δ_r . The estimated parameters from such flight data are discussed below.

case VIII (Table 2, column 3) - Combination of subcases 3-2-1-1 δ_a and δ_r with 15 measurement

noise in \hat{A}_s and \hat{B}_r ...

The estimated parameters did not show any improvement over that estimated in case 7. The estimated values of plant-model control derivatives still showed great scatter in the one estimated under case 8.

case 8 (Table 2, column 4) - Construction of modeltype 2-2-1-1 \hat{A}_s and \hat{B}_r with 25 measurements/step in \hat{A}_s and \hat{B}_r

Estimated parameters still followed the same trend in their estimated values as in case 7B1.

In this stage, difficulty of estimating control derivatives when combination of \hat{A}_s and \hat{B}_r is weak, led to idea of introducing delay between the two control inputs. As mentioned earlier, identical control inputs \hat{A}_s and \hat{B}_r would confuse the neural network and it would not be able to distinguish between \hat{A}_s and \hat{B}_r inputs. It was hoped that the delay would give a chance to neural network to distinguish between these two control inputs i.e. \hat{A}_s and \hat{B}_r . Based on this conjecture, following types of inputs were used for data generated and analysis, results of which are given in table 3.

case 9 (Table 3, column 3) - Construction of modeltype 2-2-1-1 \hat{A}_s and \hat{B}_r with rubber control delayed by 1.5 second. i.e. rubber input was increased 1 second after alarm input is applied.

The estimated parameters clearly reflected the nature of

small delay between the two inputs. Not only the control derivatives got smaller but also were very close to their true values K_{gain} being only exceptional and with consistently low standard deviation. However, stability derivatives $C_{\text{m}}/C_{\text{yp}}/C_{\text{yr}}$ and C_{ay} were still on higher side. It seemed desirable to explore and find control input form that might reduce these standard deviations.

case II (Table 3, column 4) : Combination of substep 3-2-1-1 to 3n and 3r with random control delayed by 1.0 second

Like case I, parameters were again well estimated except for some deterioration in C_{ypn} and C_{ay} values.

case III (Table 3, column 5) : Combination of substep 3-2-1-1 to 3n and 3r with random control delayed by 1.0 second.

Estimated parameters from this study plotted good estimated values for all derivatives except $C_{\text{ay}}, C_{\text{yp}}$ and C_{yr} . Overall the 1.0 second delay was rather impressive as 1.0 second delay.

In the light of the potential shown by time delay between the applications of the two control inputs, the idea was further extended wherein second control followed at the end of the first control. The following two cases were investigated towards this goal.

case IIIA (Table 4, column 3) : Combination of substep 3-2-1-1 to 3n and 3r such that random input was applied for the first, when

seconds, radial input kept zero
and for the next seven seconds,
radial input being applied keeping
axial input zero

case XY Table 4, column (i) : Combination of substep 2-2-1-1 to
and for such that radial input is
applied for the first seven seconds
and axial input for the next
seven seconds.

The estimated parameters from case XX and XY clearly
indicate that for such type of control inputs, their exists no
confusion for neural network. It can very easily distinguish
between two inputs. It was also observed that in case XY the
standard deviations were much lower. Also the above type of
application of control inputs resulted in good estimates of even
the weak derivatives like $C_{\dot{y}y}, C_{\dot{y}y}, C_{\dot{y}y}, C_{\dot{y}y}, C_{\dot{y}y}$ and $C_{\dot{y}y}$.

For illustration, specifically for case XX, the actual, the
trained and the predicted values of $C_{\dot{y}y}, C_{\dot{y}y}, C_{\dot{y}y}$ are plotted in
Fig.7a, 7b, and 7c. By actual value we mean those values of force
or moment coefficients which were calculated using eq.6.6) with
true values of parameters for particular control inputs of case
XX. As values of these force or moment coefficients were present
as output in the input-output file used to train the FFNN, the
values so obtained after training the FFNN for optimal network
parameters are termed as trained values. The predicted values are
those values which are obtained by using of the estimated
parameters in eq.6.6). It may be seen from Fig. 7 that the trained,

measured, and predicted C_L , C_m and C_p show good match, and thus reliable validation of Beta-method for predicting parameter estimates for flight data.

After integrations for all the estimated parameters are plotted in Fig. 35,36 and 36. These figures clearly indicate the near normal distribution for most of the estimated parameters and justify the concept of mean values and standard deviation for these estimated parameters.

Since the real flight data is generally noisy in nature, the effect of measurement noise on the estimated parameters was carried out to show how the accuracy of the estimates is affected by presence of measurement noise. For this purpose periodic measurement noise was added to μ, r, δ and C_L or C_m or C_p corresponding to simulated flight data of case X. The results for it are given under case IV and case VII below :

case IV (table 4, column XI) - case X + 1% measurement noise in

$$\mu, r, \delta \text{ and } C_L \text{ or } C_m \text{ or } C_p$$

case VII (table 4, column XI) - case X + 1% measurement noise in

$$\mu, r, \delta \text{ and } C_L \text{ or } C_m \text{ or } C_p$$

In case IV none of the parameters are well estimated as was observed for case X (see table). This indicates that presence of low measurement noise does not affect the accuracy of estimates and this reflects on the robustness of Beta-method. A comparison of results for IX (case IV) and XI (case VII) cases shows the increase in noise level does result in marginally poorer estimates for most of the parameters. Curiously, some of the cross derivatives like $C_{L\dot{\alpha}}$, $C_{L\dot{\beta}}$ and $C_{p\dot{\alpha}}$ are actually better estimated.

CHAPTER 5

CONCLUSIONS AND RECOMMENDATIONS

5.1 Conclusion

In the present work, Delta method using either two files used for estimation of lateral-directional parameters from simulated flight data. Different types of control inputs were used to generate corresponding sets of flight data for analysis through Delta method. Comparison of parameter estimates as obtained showed how the accuracy of estimates depends on the types of control inputs used for flight data. In particular, it was observed that a time delay between aileron and rudder control derivatives further estimation of aileron and rudder control derivatives. Further, multiple 2-D-1-D type aileron and rudder lead to better estimation of aircraft dynamics and thereby to better estimates as compared to pulse, sinusoidal or any arbitrary varying inputs. The Delta method has been found to be robust enough to provide good parameter estimates even in presence of measurement noise in the flight data.

5.2 Recommendations

It would be of great interest to estimate Delta method on real flight data. In particular, if data could be generated for different types of control inputs studied in the present work, then these could be readily compared to the results reported herein. The issue of time delay between aileron and rudder inputs is worth verifying using real flight data. In present work, force and moment coefficients have been supplied separately. It would be

allowing to integrate where C_1 , C_2 and C_3 are summed together
and then apply EM algorithm for parameter estimation.

REFERENCES

1. Socol, E., and Morris, J. J., "The Stability Derivatives of the Helios Aircraft Estimated by Various Methods and Derived from Flight Test Data," *FAA-88-714*.
2. Socol, E., "Stability and Control of Airplanes and Helicopters," Academic Press, New York, 1988.
3. Collins D.E., "USAF Stability and Control Hand Book (SCOTH)," Wright-Patterson Air Force Base, OH, Contract August 1988.
4. Hagen, E. F., and Eft, E. W., "Modification of Dynamic System - Theory and Formulation," *NASA RP 129*, Feb. 1988.
5. Pearson, A., "Determination of Aerodynamic Coefficients of the F14D 49 STD Aircraft from Flight Test by means of Manual Steady Model Matching," Paper No. 878-1987 of Publication *IEEE-TT-104*, Nov. 1978.
6. Taylor, L. W., Eft, E. W., and Powell, B. G.'s, comparison of Newton-Raphson and other Methods for Determining Stability Derivatives from Flight Data," *NASA Paper No. 48-325* May 1965.
7. Eft, E. W., "Modification Dynamic Methods," *ADAP-1.8-104*, Nov. 1978.
8. Pearson, A., "20 Years of Adaptive Neural Network Perceptrons, Backpropagation, and Backpropagation," *Proceedings of the IEEE*, Vol. 78, No. 5, Sep. 1990, pp. 1493-1498.
9. Chao, S., Jones, C. P. R., "Turbulent Boundary Evolution

1. "Error Algorithm for Training Layered Networks," Vol. 1, Control, 1993, Vol. 30, No. 4, pp. 628-638.
10. Chen, S., Billings, S. A., and Grant, P. M., "Nonlinear System Identification Using Neural Networks," Vol. 1, Control, 1990, Vol. 27, No. 4, pp. 689-698.
11. Sjöberg, J., Eklund, B., and Ljung, L., "Neural Networks in System Identification," Proceedings of the 1991 IFAC Symposium on System Identification, 4-8 July 1991, Copenhagen, Denmark, Vol. 3, pp. 49-51.
12. Hess, B. A., "On the Use of Backpropagation with Feed Forward Neural Networks for the Aerodynamic Estimation Problem," AIAA-90-2624-CP, 1990.
13. Youcef, H. H., "Estimation of Aerodynamic Coefficients using Neural Networks," AIAA paper 90-2670, Aug. 1990.
14. Saadawi, and Jangpanjar, B. T., "Aspects of Feed Forward Neural Network Modeling and Its Application to Lateral - Directional Flight Data," AIAA 88-2670, Sep. 1990.
15. Saad, S. B. and Jangpanjar B. T., "Aircraft Parameter Estimation Using Recurrent Neural Networks - A critical appraisal," AIAA Paper 90-2674-a, Aug. 1990.
16. Liem, D. J., and Siegel, R. F., "Identification of Aerodynamic Coefficients Using Computational Neural Networks," Journal of Guidance Control and Dynamics, Vol. 16, No. 4, Oct-Dec. 1993, pp. 628-635.
17. Balighatani S.C., Clark A.E. and Fahn P.B., "Time Series Techniques For Aircraft Parameter Estimation Using Neural

18. Jategaake R. "Identification of the Adaptive Model of the DLR Research Aircraft STIAS from Flight Test Data" DLR-4700-90, Sept. 1990
19. Robert Ruder . "Parameter Estimation from Flight Data Using Feed Forward Neural Networks" AIAA Thirtieth Aerospace Engineering Conference, February '90

TABLE 1

Parameter	True Value	Estimated Parameters				
		case1	case2	case3	case4	case5
$-C_{1p}$	0.79	$1.1^{+0.14}_{-0.14}$	0.77	0.80	0.50	0.70
C_{2p}	0.42	$0.40^{+0.13}_{-0.13}$	0.40	0.44	-0.17	0.30
$-C_{3p}$	0.126	0.075	0.101	0.102	0.09	0.11
$-C_{4p}$	0.23	0.26	ME	0.22	0.12	0.074
C_{5p}	0.044	ME	0.044	ME	ME	-0.10
			(0.000)			(0.000)
$-C_{6p}$	0.133	0.14	0.14	0.07	0.04	0.10
		(0.040)	(0.100)	(0.001)	(0.001)	(0.090)
$-C_{7p}$	0.075	0.44	0.77	0.12	0.24	0.40
		(0.070)	(0.120)	(0.000)	(0.020)	(0.170)
C_{8p}	0.20	0.25	0.20	0.18	0.21	0.14
		(0.040)	(0.001)	(0.070)	(0.040)	(0.001)
C_{9p}	0.0	0.004	ME	-0.004	0.000	-0.007
		(0.000)		(0.000)	(0.000)	(0.001)
$-C_{10p}$	0.10	ME	0.10	ME	ME	-0.20
			(0.001)			(0.001)

C_{20}	0.20	0.43	1.13	0.19	0.47	-0.000
		00.191	11.331	00.013	10.131	00.041
C_{21}	0.727	0.33	0.04	-0.00	0.00	0.07
		01.00	10.401	11.00	10.01	10.001
$-C_{22}$	1.133	0.40	0.33	0.00	0.00	1.1
		00.001	10.101	10.000	10.001	00.101
C_{23a}	0.00	0.000	NE	0.000	0.07	0.000
		00.001		00.000	10.001	00.001
C_{23b}	0.10	NE	0.00	NE	NE	0.10
			10.000			10.001

0 = standard deviation

NE = not estimated

Table 2

Parameter	True Value	Estimated Parameters			
		case0	case1	case2	case3
$-C_{1p}$	0.90	1.1 (0.21) ^B	0.91 (0.11)	0.92 (0.05)	0.93 (0.10)
C_{1r}	0.42	0.42 (0.07)	0.41 (0.12)	0.50 (0.18)	0.50 (0.20)
$-C_{2p}$	0.120	0.094 (0.03)	0.121 (0.03)	0.11 (0.03)	0.21 (0.07)
$-C_{2r}$	0.22	0.25 (0.05)	0.209 (0.04)	0.095 (0.03)	0.20 (0.03)
C_{3dr}	0.000	0 (0.01)	0.00 (0.01)	0.009 (0.005)	0.00 (0.004)
$-C_{sp}$	0.105	0.10 (0.04)	0.09 (0.14)	0.10 (0.04)	0.10 (0.08)
$-C_{ss}$	0.405	0.35 (0.10)	0.44 (0.19)	0.40 (0.10)	0.40 (0.17)
C_{sp}	0.20	0.27 (0.08)	0.20 (0.05)	0.20 (0.04)	0.20 (0.09)
C_{ssr}	0.0	-0.004 (0.003)	0.000 (0.004)	-0.001 (0.003)	-0.005 (0.005)
β	0.10	0 (0.01)	0.09 (0.04)	-0.008 (0.003)	-0.005 (0.004)

C_{3P}	0.38	0.38	0.38	-0.003	-0.003
		10.000	10.000	10.000	10.000
C_{3P}	0.107	1.42	0.38	0.27	0.29
		10.000	10.000	10.000	10.000
$-C_{3B}$	1.133	0.97	1.97	1.1	1.1
		10.000	10.000	10.000	10.000
C_{3B2}	0.03	0.08	0.028	0.000	0.005
		10.000	10.000	10.000	10.000
C_{3B2}	0.19	NE	0.08	0.10	0.10
			10.000	10.000	0.000

0 = standard deviation

NE = not estimated

Table 1: 3

Parameter	True Value	Estimated Parameters		
		case10	case11	case12
$-C_{1P}$	0.00	1.00 (0.19) ^B	1.00 (0.14)	0.99 (0.11)
C_{1P}	0.40	0.40 (0.09)	-0.00 (0.10)	0.37 (0.07)
$-C_{1B}$	-0.00	0.40 (0.09)	0.10 (0.09)	0.10 (0.09)
$-C_{1dB}$	0.00	0.00 (0.04)	0.00 (0.04)	0.00 (0.03)
C_{1dP}	0.00	0.00 (0.00)	0.00 (0.00)	0.00 (0.00)
$-C_{2P}$	0.10	0.10 (0.04)	-0.00 (0.04)	0.00 (0.00)
$-C_{2B}$	0.00	0.00 (0.10)	0.00 (0.00)	0.00 (0.10)
C_{2d}	0.00	0.00 (0.04)	0.00 (0.04)	0.00 (0.04)
C_{2dB}	0.0	0.00 (0.00)	0.00 (0.00)	-0.00 (0.00)
$-C_{2dP}$	0.00	0.10 (0.00)	0.10 (0.00)	0.00 (0.00)

C_{20}	0.30	0.30	-0.002	0.343
		(0.375)	(0.389)	(0.439)
C_{21}	0.197	0.79	-0.34	0.93
		(0.820)	(0.875)	(1.040)
$-C_{28}$	1.033	1.04	1.09	1.03
		(0.179)	(0.345)	(0.171)
C_{30a}	0.03	0.011	0.004	0.004
		(0.040)	(0.000)	(0.071)
C_{30c}	0.19	0.19	0.22	0.243
		(0.060)	(0.11)	(0.081)

σ = standard deviation

Table 1: 4

Parameter	True Value	Calculated		Percentage	
		error(%)	error(%)	error(%)	error(%)
$-C_{1F}$	0.99	1.00	0.99	1.00	1.00
		$(0.11)^{+0.01}_{-0.01}$	(0.00)	(0.17)	(0.20)
C_{1F}	0.40	0.39	0.40	0.40	0.40
		(0.00)	(0.00)	(0.00)	(0.00)
$-C_{1B}$	0.109	0.10	0.10	0.10	0.1
		(0.02)	(0.004)	(0.00)	(0.00)
$-C_{2B}$	0.00	0.00	0.00	0.00	0.00
		(0.00)	(0.000)	(0.00)	(0.00)
C_{2BF}	0.000	0.000	0.000	0.00	0.00
		(0.000)	(0.000)	(0.000)	(0.00)
$-C_{2F}$	0.000	0.00	0.00	0.00	0.000
		(0.07)	(0.04)	(0.00)	(0.00)
$-C_{2B}$	0.000	0.00	0.00	0.00	0.00
		(0.00)	(0.00)	(0.00)	(0.00)
C_{2B}	0.00	0.00	0.00	0.00	0.00
		(0.00)	(0.00)	(0.00)	(0.00)
C_{2BF}	0.00	-0.001	0.00	0.000	0.000
		(0.000)	(0.00)	(0.000)	(0.00)
$-C_{2BF}$	0.00	0.00	0.00	0.00	0.00
		(0.000)	(0.00)	(0.00)	(0.00)

$-C_{22}$	0.360	0.348	0.346	0.344	0.332
		10.183	00.000	00.000	10.000
$-C_{23}$	0.737	0.693	0.648	0.603	0.775
		10.101	00.000	00.000	10.000
$-C_{24}$	1.120	1.111	1.111	1.000	1.000
		10.000	00.000	00.000	10.000
C_{33a}	0.000	0.007	0.000	0.000	0.000
		10.000	10.000	00.000	10.000
C_{34a}	0.119	0.011	0.119	0.119	0.119
		00.000	10.000	10.000	00.000

0 = standard deviation

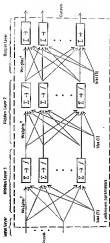


Fig. 2 Feed forward neural network with two hidden layers

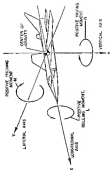


FIG. 3 Steiner's Axis System

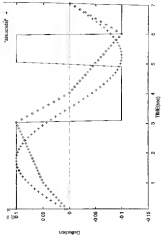


Fig. 4 Three Types of Control Input Form

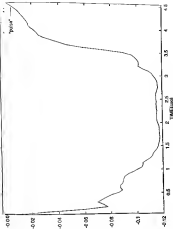


Fig. 5 Pulse type evolution (input power 500)

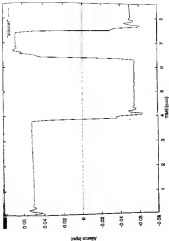


FIG. 10. Radius change (calculated) at various times (signal) (Source: 10.10)

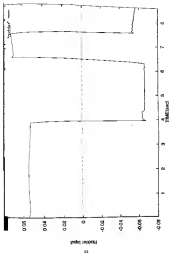


Fig. 10. output signal of the system (same with Fig. 9)

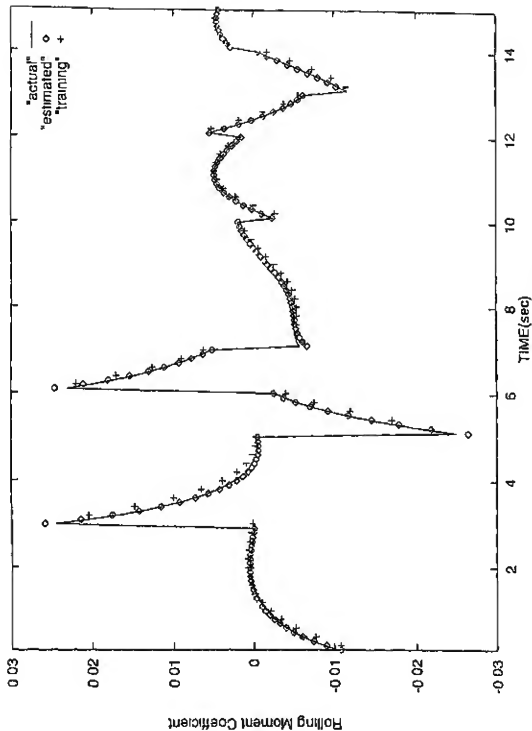


FIG 7A Comparison Of Actual Trained and Estimated
Response Of Rolling Moment Coefficient (C_l)

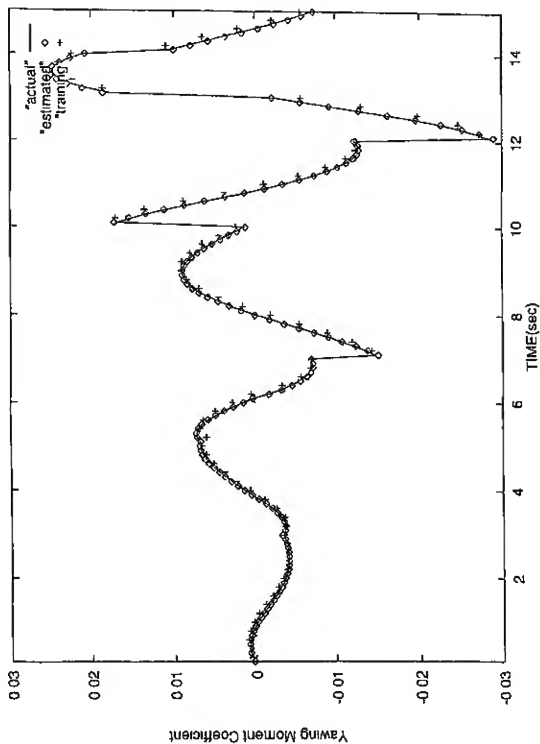


FIG 7b Comparison of Actual Trained and Estimated
Response Of Yawing Moment Coefficient (C)

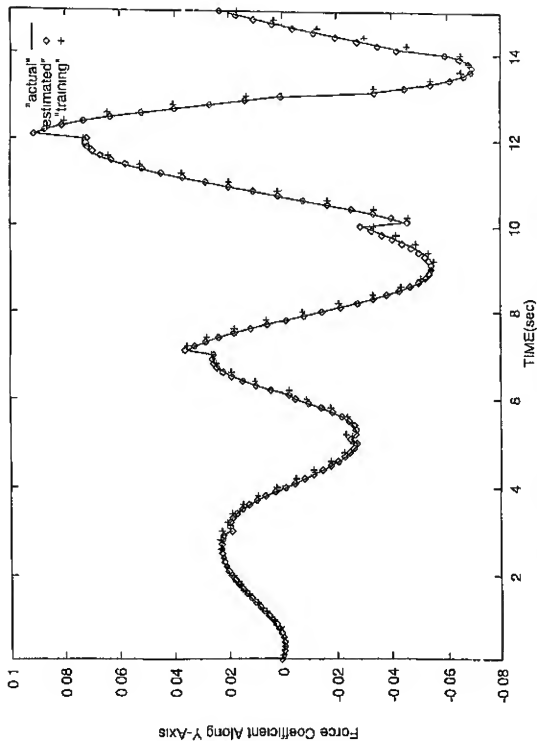


FIG 7C Comparison Of Actual Trained and Estimated
 Response Of Force Coefficient Along Y-axis (C_y)



Fig. 8 - Histograms for Estimated Parameters C_{gp} , C_{dr} , C_{ga} , C_{gd} and C_{dp} .

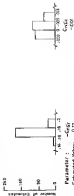
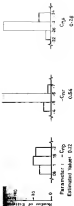


Fig. 8.4- Histograms for Estimated Parameters C_{mp} , C_{mr} , C_{mg} , C_{mr} , C_{mp} , C_{mg}



Fig. 8c. Histograms for Estimated Parameters C_{yp} , C_{pr} , C_{ys} , C_{ysr} and C_{yr} .